

Solid-State NMR Characterization of the Surfactant–Silica Interface in Templated Silicas: Acidic versus Basic Conditions

Niki Baccile,[†] Guillaume Laurent,[†] Christian Bonhomme,[†] Plinio Innocenzi,[‡] and Florence Babonneau^{*,†}

Laboratoire de Chimie de la Matière Condensée de Paris, Université Pierre et Marie Curie-Paris6 and CNRS, 4 Place Jussieu, 75252 Paris Cedex 05, France, and Dipartimento di Architettura e Pianificazione, Laboratorio di Scienza dei Materiali e Nanotecnologie, Università di Sassari and INSTM, Palazzo Pou Salit, Piazza Duomo 6, 07041 Alghero Sassari, Italy

Received October 25, 2006. Revised Manuscript Received January 12, 2007

A combination of one-dimensional and two-dimensional solid-state magic angle spinning nuclear magnetic resonance (MAS NMR) experiments has been used to investigate the hybrid organic–inorganic interfaces in surfactant templated silicas. Samples prepared with cetyltrimethylammonium bromide (CTAB) under acidic (HCl) and basic (NaOH) conditions have been compared. The use of sequences based on the ²⁹Si–¹H heteronuclear dipolar interactions allows us to selectively filter the NMR response of the protons close to the Si surface sites showing directly the clear difference between the two systems. The basic sample is characterized by a small amount of Si–OH groups and a short distance between the Si–O[−] surface groups and the surfactant polar head group, while the acidic sample exhibits a silanol-rich surface with a longer distance between the Si surface sites and the polar head groups. The nature of the interface induces consequent differences in the structure of the adsorbed water layers present at the interface, and this has been revealed by near-infrared experiments, as well as ¹H MAS NMR spectra recorded on dehydrated and partially rehydrated samples. One objective of this work was also to show that the use of standard solid-state NMR conditions (magnetic field of 7 T and magic angle spinning frequency of less than 15 kHz) can be largely sufficient to obtain extremely valuable information regarding the silica–surfactant interfaces.

Introduction

In the past 15 years, a large number of studies has been focused on long-range ordered mesoporous materials obtained in solution through the self-assembly of a variety of amphiphilic templating agents with a growing inorganic phase.¹ Their structural characteristics (high surface area, tunable geometry of the porous network, narrow pore size distribution)² combined with the possibility to process them in various shapes³ (calibrated spherical powders,⁴ thin films,⁵ membranes, monoliths⁶) make them extremely attractive for a wide range of applications in the fields of catalysis,^{7–9} chromatography,¹⁰ drug release,¹¹ sensors,¹² electronics,¹³ or

the environment.^{14,15} Moreover, the large versatility associated with a relative simplicity of the synthetic protocols has certainly contributed to the immediate interest of the community of chemists for this class of materials. Just by playing with experimental parameters such as the inorganic precursor, the type of surfactant, the pH of the solution, the temperature, the nature of cosolvent etc., mesoporous materials with a large range of nanostructures can be synthesized.

Despite this abundant literature, relatively few studies have been focused on a detailed characterization of the interactions that develop between the structuring agents and the inorganic species. These interactions are of key importance to drive the self-assembly process and to lead to the formation of a given silica–surfactant mesophase. Several research groups have focused on the understanding of the formation mechanism, and reviews are dedicated to these topic, not only in the case of powders obtained through precipitation^{16,17} but

* Corresponding author. E-mail: fb@ccr.jussieu.fr.

[†] Université Pierre et Marie Curie-Paris6 and CNRS.

[‡] Università di Sassari and INSTM.

- (1) (a) Schuth, F. *Stud. Surf. Sci. Catal.* **2001**, *135*, 1. (b) Tanev, P.; Butruille, J.-R.; Pinnavaia, T. J. *Chemistry of Advanced Materials: An Overview*; Wiley-VCH: Weinheim, Germany, 1998.
- (2) Soler-Illia, G. J. de A. A.; Sanchez, C.; Lebeau, B.; Patarin, J. *Chem. Rev.* **2002**, *102*, 4093.
- (3) Zhao, D.; Yang, P.; Huo, Q.; Chmelka, B. F.; Stucky, G. D. *Curr. Opin. Solid State Mater. Sci.* **1998**, *3*, 111.
- (4) (a) Lu, Y.; Fan, H.; Stump, A.; Ward, T. L.; Rieker, T.; Brinker, C. J. *Nature* **1999**, *398*, 223. (b) Baccile, N.; Grosso, D.; Sanchez, C. J. *Mater. Chem.* **2003**, *13*, 3011.
- (5) (a) Brinker, C. J.; Lu, Y.; Sellinger, A.; Fan, H. *Adv. Mater.* **1999**, *11*, 579. (b) Grosso, D.; Babonneau, F.; Albouy, P. A.; Amenitsch, H.; Balkenende, A. R.; Brunet-Bruneau, A.; Rivory, J. *Chem. Mater.* **2002**, *14*, 931.
- (6) Melosh, N. A.; Lipic, P.; Bates, F. S.; Wudl, F.; Stucky, G. D.; Fredrickson, G. H.; Chmelka, B. F. *Macromolecules* **1999**, *32*, 4332.
- (7) Sayari, A. *Chem. Mater.* **1996**, *8*, 1840.
- (8) Corma, A. *Chem. Rev.* **1997**, *97*, 2373.

- (9) Goettmann, F.; Grosso, D.; Mercier, F.; Mathey, F.; Sanchez, C. *Chem. Commun.* **2004**, *10*, 1240.
- (10) Ciesla, U.; Schuth, F. *Microporous Mesoporous Mater.* **1999**, *27*, 131.
- (11) (a) Vallet-Regi, M.; Ramila, A.; del Real, R. P.; Perez-Pariente, J. *Chem. Mater.* **2001**, *13*, 308. (b) Vallet-Regi, M. *Chem.—Eur. J.* **2006**, *12*, 5934.
- (12) Nicole, L.; Boissière, C.; Grosso, D.; Hesemann, P.; Moreau, J.; Sanchez, C. *Chem. Commun.* **2004**, 2312.
- (13) Balkenende, A. R.; de Theije, F. K.; Kriege, J. C. K. *Adv. Mater.* **2003**, *15*, 139.
- (14) Antochshuk, V.; Olkhovik, O.; Jaroniec, M.; Park, I.-S.; Ryoo, R. *Langmuir* **2003**, *19*, 3031.
- (15) Reddy, E. P.; Sun, B.; Smirniotis, P. G. *J. Phys. Chem. B* **2004**, *108*, 17198.

also in the case of thin films prepared via evaporation-induced self-assembly.^{17,18} Less work has been centered on the description of the inorganic–organic interfaces in the final materials. Nevertheless, the way the templating molecules interact with the inorganic walls strongly influences important structural features. Upon removal of the surfactant species, an ordered mesoporous inorganic solid can result, whose typically amorphous framework structure is a replica of the hydrophilic mesophase regions and whose pores are vestiges of the hydrophobic components. Consequently, if hydrophilic parts of the structuring agents are embedded in the inorganic framework during the condensation step, then microporosity can be created. This has been already illustrated with the synthesis of mesoporous SBA-15 silica that uses the P123 poly(ethylene oxide)–poly(propylene oxide)–poly(ethylene oxide) block copolymer (EO₂₀–PO₇₀–EO₂₀). Galarneau et al. have shown that for a synthesis temperature below 95 °C, the SBA-15 sample presents microporosity. This was explained by the presence of polyethylene oxide PEO chains at the surface of the micellar aggregates that are lately embedded in the silica network, leading to the formation of micropores after removal of the template.^{19,20}

A key technique to investigate the organic–inorganic interfaces is high-resolution solid-state NMR. The cross-polarization (CP) sequence, based on through-space heteronuclear dipolar interactions, allows probing spatial proximities between the protons of the templating molecules and the selected nuclei present at the pore surface. Chmelka et al. very nicely illustrated this by using two-dimensional (2-D) ²⁹Si{¹H} as well as ²⁷Al{¹H} heteronuclear correlation (HETCOR) experiments to investigate the distribution of PEO and polypropylene oxide PPO copolymer blocks within the silica matrix,²¹ the aluminum incorporation in MCM-41 mesophases,^{6,22} as well as the molecular proximities between the structure-directing surfactant molecules and the crystal-like silicate sheets in layered silicate surfactant mesophases.²³ One can also use high-resolution ¹H MAS NMR and the associated double quantum (DQ) NMR spectroscopy to look for proximities between the Si–OH surface sites and the template molecules. Because of the high sensitivity of such NMR experiments, Alam et al. applied them to silicate thin films templated with the non-ionic surfactant Brij 56, a polyoxyethylene(10) cetyl ether, and demonstrated a close spatial contact between the surfactant and the silica framework, through Si–O–H···O–CH₂ proximities.²⁴ Additionally, some studies have been focused on the behavior of the

surfactant molecules using ¹³C NMR experiments.^{25,26} Experiments that look at the relative spatial arrangement of the amphiphilic templates with respect to the silica framework are thus quite scarce since most of the solid-state NMR characterization concerns the porous samples after removal of the templating agents.²⁷

In this work, we have chosen to investigate the solid-state NMR responses of two silica–surfactant mesophases characterized by the same 2-D hexagonal (*P6m*) symmetry, prepared with the same templating agent, cetyltrimethylammonium bromide (CTAB), but one under acidic (HCl) conditions and one under basic (NaOH) conditions. They correspond to the so-called SBA-3-²⁸ and MCM-41-type²⁹ silicas, respectively. Because of different synthesis pathways, the proposed interaction mechanisms are different.³⁰ In basic medium, a direct S⁺I[−] interaction is proposed between the positively charged surfactant (S⁺) and the negatively charged silica matrix (I[−]). In acidic medium, interactions with surfactant micelles are mediated by a negatively charged counterion (X[−]), whose presence is demonstrated by elemental analysis.³⁰ The interaction would be of type S⁰X[−]I⁺, which accounts for a direct charge neutralization between the counterion and the surfactant. Indeed, the weak interaction that is assumed between the template and the silica framework in these samples is in agreement with the mild conditions required to remove the surfactant (reflux in ethanol) as compared to the necessity to use acidic conditions when working with MCM-41-type systems.³⁰ Once again, this example illustrates the importance of a good understanding of the silica–surfactant interfaces in the as-prepared samples. Our objective was thus to see whether NMR techniques could be sensitive to the different silica–surfactant interaction mechanisms that have been proposed in the literature and that assume longer distances between the surfactant polar head group and the silica surface when acidic conditions are used instead of basic conditions. Indeed, to our knowledge, no detailed study has been published concerning interactions in the final material, between silica and cationic surfactants, like quaternary ammonium salts, although such templating agents have been widely used to prepare ordered mesoporous materials.

Preliminary 2-D ²⁹Si{¹H}–HETCOR experiments have been recorded on both types of samples, and different NMR responses were obtained.³¹ Two contact times—time during which the magnetization transfer occurs between the ¹H and the ²⁹Si spin systems—were used to explore increasing internuclei distances; these 2-D experiments are quite time-consuming especially with a moderate static magnetic field,

(16) Ying, J. Y.; Mehnert, C. P.; Wong, M. S. *Angew. Chem., Int. Ed.* **1999**, *38*, 56.

(17) Patarin, J.; Lebeau, B.; Zana, R. *Curr. Opin. Colloid Interface Sci.* **2002**, *7*, 107.

(18) Brinker C. J.; Dunphy, D. R. *Curr. Opin. Colloid Interface Sci.* **2006**, *11*, 126.

(19) Galarneau, A.; Cambon, H.; Di Renzo, F.; Ryoo, R.; Choib, M.; Fajula, F. *New J. Chem.* **2003**, *27*, 73.

(20) Galarneau, A.; Cambon, H.; Di Renzo, F.; Fajula, F. *Langmuir* **2001**, *17*, 8328.

(21) Janicke, M. T.; Landry, C. C.; Christiansen, S. C.; Kumar, D.; Stucky, G. D.; Chmelka, B. F. *J. Am. Chem. Soc.* **1998**, *120*, 6940.

(22) Janicke, M. T.; Landry, C. C.; Christiansen, S. C.; Birtalan, S.; Stucky, G. D.; Chmelka, B. F. *Chem. Mater.* **1999**, *11*, 1342.

(23) Christiansen, S. C.; Zhao, D.; Janicke, M. T.; Landry, C. C.; Stucky, G. D.; Chmelka, B. F. *J. Am. Chem. Soc.* **2001**, *123*, 4519.

(24) Alam, T. M.; Fan, H. *Macromol. Chem. Phys.* **2003**, *204*, 2023.

(25) Simonutti, R.; Comotti, A.; Bracco, S.; Sozzani, P. *Chem. Mater.* **2001**, *13*, 771.

(26) Alonso, B.; Massiot, D. *J. Magn. Reson.* **2003**, *163*, 347.

(27) Trebosc, J.; Wiench, J. W.; Huh, S.; Lin, V. S. Y.; Pruski, M. *J. Am. Chem. Soc.* **2005**, *127*, 3057.

(28) Huo, Q.; Margolese, D. I.; Stucky, G. D. *Chem. Mater.* **1996**, *8*, 1147.

(29) Beck, J. S.; Vartuli, J. C.; Roth, W. J.; Leonowicz, M. E.; Kresge, C. T.; Schmitt, K. D.; Chu, C. T. W.; Olson, D. H.; Sheppard, E. W. *J. Am. Chem. Soc.* **1992**, *114*, 10834.

(30) Huo, Q.; Margolese, D. I.; Ciesla, U.; Feng, P.; Gier, T. E.; Sieger, P.; Leon, R.; Petroff, P. M.; Schüth, F.; Stucky, G. D. *Nature* **1994**, *368*, 317.

(31) Baccile, N.; Maquet, J.; Babonneau, F. *C. R. Chimie* **2006**, *9*, 478.

Table 1. Structural Parameters Related to CTAB/HCl and CTAB/OH Samples: Cell Parameter (*a*), Chemical Composition from Elemental Analysis Data, and Distribution of Si Sites from ²⁹Si MAS NMR Experiments^a

| sample | <i>a</i> (Å) | N/Si (mol %) | Cl/N (mol %) | Br/N (mol %) | Q ₄ | | Q ₃ | | Q ₂ | |
|----------|--------------|--------------|--------------|--------------|----------------|----|----------------|----|----------------|---|
| | | | | | δ (ppm) | % | δ (ppm) | % | δ (ppm) | % |
| CTAB/OH | 42.4 | 0.18 ± 0.01 | 0.86 ± 0.03 | 0.05 ± 0.01 | −110.3 | 43 | −100.9 | 50 | −91.2 | 7 |
| CTAB/HCl | 41.4 | 0.21 ± 0.01 | | 0.08 ± 0.02 | −109.2 | 48 | −99.2 | 43 | −90.5 | 9 |

^a Error margins in ²⁹Si NMR quantitative analysis are estimated to ±1%.

which limits the number of possible contact times. Indeed, in most of the previous publications, only one experiment recorded at only one contact time has been presented. Considering the valuable information that can be extracted from these experiments with a variation of contact times, we have developed a new sequence based on a double CP transfer, a first transfer from ¹H to ²⁹Si, to select the Si sites close to protons, and essentially the surface sites, and then a second transfer back from ²⁹Si to ¹H to detect only the signal of the protons that are dipolar coupled to these surface sites. Since it is a 1-D sequence, a complete variation of contact times can be recorded that allows exploring in a quasi-continuous way the proximities between ¹H and ²⁹Si nuclei. Additional ¹H MAS NMR experiments have been recorded with high spinning frequency on dehydrated and partially rehydrated samples to look at the adsorbed water layers, while near-infrared experiments, which are very sensitive to the extent of hydrogen bonding involving water molecules, have completed the series of characterizations of the silica–surfactant interfaces of these two samples.

Experimental Procedures

Material Synthesis. The CTAB/OH sample was prepared with the following conditions: 0.15 g of CTAB (C₁₆H₃₃N⁺(CH₃)₃Br[−]; Aldrich) was dissolved in a 3.85 wt % NaOH aqueous solution (8 g of NaOH in 200 mL of water). The solution was stirred until all surfactant was dissolved. A total of 0.72 g of TEOS (tetraethoxysilane; Fluka) was then added to the mixture under stirring. The final molar ratios were TEOS/CTAB/NaOH/H₂O = 1:0.12:0.5:120. The stirring of the solution (~500 rpm) was continued for 3 h and then filtered and dried for 1 day at ambient conditions and finally in the oven overnight at 100 °C.

The synthesis of the CTAB/HCl sample follows the same steps. A total of 0.10 g of CTAB was dissolved in an acidic aqueous solution composed of 0.12 g of water and 6.27 g of a 12.63 wt % (4 mol L^{−1}) HCl aqueous solution. The mixture was stirred for a few minutes before adding 0.5 g of TEOS. The final molar ratios were TEOS/CTAB/HCl/H₂O = 1:0.12:9.2:130. The filtering and the double drying processes were the same as in the CTAB/OH case.

Solid-State NMR Spectroscopy. ²⁹Si MAS NMR spectra were recorded on a Bruker AVANCE 400 (9.40 T) spectrometer. The 7 mm zirconia rotors spinning at 5 kHz were employed. A total of 324 transients were collected with a 90° pulse of 6.5 μs and recycle delays of 200 s (CTAB/HCl) and 500 s (CTAB/OH). These values were chosen according to previous works found in the literature.^{32,33} Spectra were fitted with DMFIT2004 software.³⁴ ¹H MAS NMR spectra were recorded on a Bruker AVANCE 400 spectrometer with

a 2.5 mm zirconia rotor and with a spinning frequency of 30 kHz. Eight transients were collected with a 90° pulse of 3 μs and a recycling delay of 5 s. The chemical shift reference for the ¹H and ²⁹Si NMR experiments was tetramethylsilane (TMS; δ = 0 ppm).

2-D ²⁹Si{¹H} heteronuclear correlation (HETCOR) experiments and double cross-polarization ¹H-²⁹Si-¹H experiments were recorded on a Bruker Avance 300 spectrometer with a CP-MAS probe and a 4 mm rotor spinning at 14 kHz. For the CP-HETCOR experiments, polarization transfer was achieved by applying a constant radio frequency (RF) field on the ²⁹Si channel ($\nu_{RF}^{(29Si)} = 50$ kHz) while the RF field on the ¹H channel was ramped ($\nu_{RF}^{(1H)} = 50 \pm 14$ kHz). For the double CP experiments (sequence described in the text), cross-polarization transfers were performed under adiabatic tangential ramps^{35,36} to enhance the signal with respect to other known methods.³⁷ The pulse phasing was $\phi_1 = (x, x, -x, -x)$, $\phi_2 = (-x, -x, x, x)$, $\phi_3 = (x, -x)$, $\phi_4 = (x, x, x, x, -x, -x, -x, -x, y, y, y, y, -y, -y, -y, -y)$, $\phi_5 = (x, -x, x, -x, -x, x, -x, x, y, -y, y, -y, -y, y, -y, y)$. The efficiency of the sequence was carefully verified before each experiment by setting the RF field on the X channel to 0 and to ensure that no ¹H signal was detected. For all experiments, two-pulse phase-modulated (TPPM) proton decoupling was applied during acquisition.³⁸ Quadrature detection in *t*₁ was realized using the STATES method.³⁹ Experimental conditions for the individual NMR experiments varied and are presented in detail in the figure captions accompanying the respective spectra.

Other Analyses. X-ray diffraction patterns were recorded with a Philips PW 1830 diffractometer equipped with a Cu–Kα source (λ = 1.54 Å), with a 0.02° step and an acquisition time of 5 s per point.

Elemental analysis was performed at the CNRS Centre d'Analyse Élémentaire, Vernaison, France.

Infrared absorption spectra were measured by a Fourier transform infrared (FT-IR) spectrophotometer (Nicolet Nexus) mounted with a KBr-DTGS detector, in the 4000–400 cm^{−1} range (256 scans with a 4 cm^{−1} resolution). Near-infrared (NIR) spectra were measured in the 9000–4500 cm^{−1} range, using 256 scans with a 4 cm^{−1} resolution. The spectra were recorded in absorption using anhydrous KBr powder, and the background was recorded using a KBr pellet prepared in the same conditions. These experimental conditions assured that the effect of water absorption in KBr pellets from the external environment did not appear in the infrared spectra. The beam splitter was CaF₂, and the detector was made of InGaAs.

(32) Steel, A.; Carr, S. W.; Anderson, M. W. *Chem. Mater.* **1995**, *7*, 1829.

(33) Goletto, V. Synthèse et Caractérisation d'Organosilices Mésostructurées à Porosité Périodique. Ph.D. Thesis, Université Pierre et Marie Curie-Paris6, Paris, 2002.

(34) Massiot, D.; Fayon, F.; Capron, M.; King, I.; Le Calve, S.; Alonso, B.; Durand, J.-O.; Bujoli, B.; Gan, Z.; Hoatson, G. *Magn. Reson. Chem.* **2002**, *40*, 70.

(35) Hediger, S.; Meier, B. H.; Kurur, N. D.; Bodenhausen, G.; Ernst, R. R. *Chem. Phys. Lett.* **1994**, *223*, 283.

(36) Hediger, S.; Meier, B. H.; Ernst, R. R. *Chem. Phys. Lett.* **1995**, *240*, 449.

(37) Christiansen, S. C.; Hedin, N.; Epping, J. D.; Janicke, M. T.; del Amo, Y.; Demarest, M.; Brzezinski, M.; Chmelka, B. F. *Solid State Nucl. Magn. Res.* **2006**, *29*, 170.

(38) Bennett, A. E.; Rienstra, C. M.; Auger, M.; Lakshmi, K. V.; Griffin, R. G. *J. Chem. Phys.* **1995**, *103*, 6951.

(39) States, D. J.; Haberkorn, R. A.; Ruben, D. J. *J. Magn. Reson.* **1982**, *48*, 286.

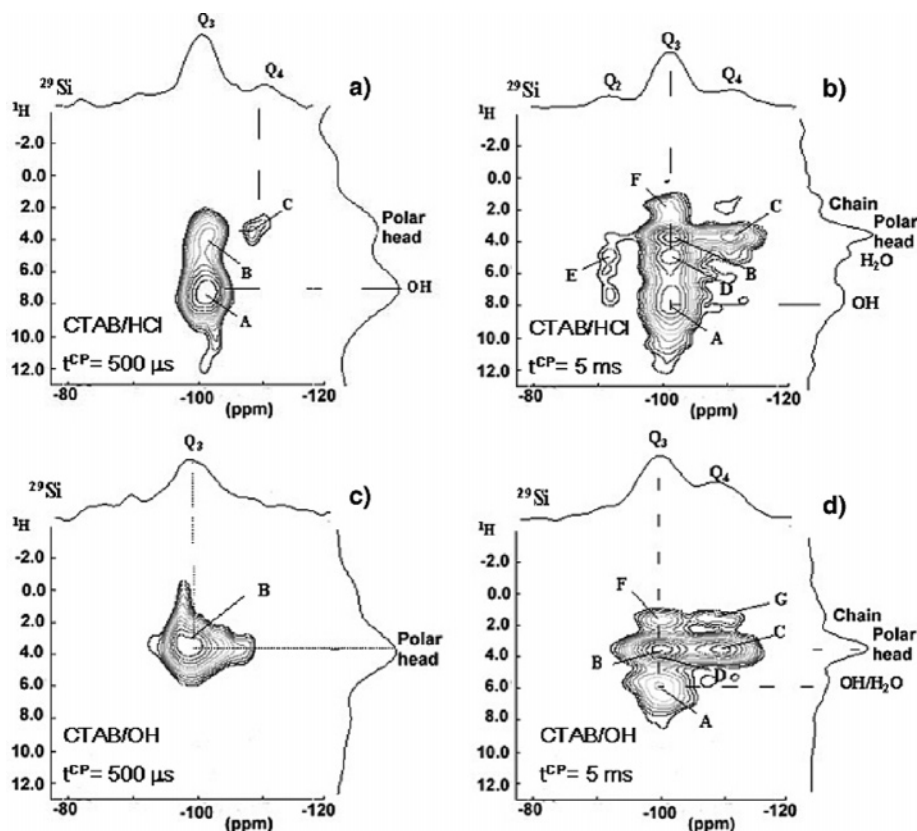


Figure 1. Two-dimensional HETCOR $^{29}\text{Si}\{^1\text{H}\}$ spectra recorded on CTAB/HCl with $\tau_{\text{CP}} = 500 \mu\text{s}$ (a) and $\tau_{\text{CP}} = 5 \text{ms}$ (b) and on CTAB/NaOH with $\tau_{\text{CP}} = 500 \mu\text{s}$ (c) and $\tau_{\text{CP}} = 5 \text{ms}$ (d). Experimental parameters (number of transients, NS, and number of slices in second dimension, TD1) are the following: (a) NS = 800, TD1 = 94; (b) NS = 904, TD1 = 32; (c) NS = 2144, TD1 = 32; and (d) NS = 904, TD1 = 64. t_1 increment was set to $66.7 \mu\text{s}$ for all experiments. Contour level base has been chosen from maximum and up to noise level.

Results

Characterization of the Silica–Surfactant Bulk Powders. The two samples CTAB/HCl and CTAB/OH have been characterized by X-ray diffraction, elemental analysis, and ^{29}Si MAS NMR. The results are summarized in Table 1. Both samples have a 2-D hexagonal structure ($P6m$) with very similar cell parameters (42.4 \AA for CTAB/HCl and 41.4 \AA for CTAB/OH). Elemental analysis reveals a higher surfactant–Si molar ratio in the final powders (0.18 for CTAB/HCl and 0.21 for CTAB/OH) as compared to the starting nominal composition (0.12). Under acidic conditions, an almost complete anionic exchange took place with the incorporation of 0.86 Cl^- and only 0.05 Br^- in CTAB/HCl. The amount of anions ($(\text{Br} + \text{Cl})/\text{N} = 0.91$) almost compensates the positive charge of the surfactant polar head group, which results in a fairly low expected charge on the silica network. This has already been noticed in the literature, as mentioned in the Introduction.³⁰ On the contrary, the amount of residual anions in CTAB/OH is extremely low ($\text{Br}/\text{N} = 0.08$) and in good agreement with a direct electrostatic interaction between the positively charged polar head group and the negatively charged silicate species.

The ^{29}Si MAS NMR spectra present peaks due to the three different silicon sites: $\text{Q}_4 = \text{SiO}_2$, $\text{Q}_3 = \text{SiO}_{1.5}\text{Ot}$, and $\text{Q}_2 = \text{SiO}(\text{Ot})_2$ (Ot: nonbridging oxygen).³¹ The number of Q_3 sites is high in both samples because of the rather short aging time of the powder after precipitation (3 h). ^{13}C MAS NMR spectra (not shown) have confirmed the absence of any residual ethoxy groups. One might expect that under acidic

conditions, the Q_3 units thus correspond to the presence of Si–OH groups, 0.64 per Si (including Q_3 and Q_2 contributions). Under basic conditions, a majority of Si–O[−] groups were expected, but some Si–OH groups might also be present in the silica network. The percentage of each Si site (Table 1) shows that in basic medium (CTAB/OH), the network is slightly more condensed than in acidic medium (CTAB/HCl), a well-known result of sol–gel chemistry.⁴⁰

The ^1H MAS NMR spectra of CTAB/HCl and CTAB/OH (see Supporting Information) show three main peaks at $\delta_{\text{iso}} = 0.9, 1.3,$ and 3.3 ppm , respectively, attributed to alkyl chain CH_3 protons, alkyl chain CH_2 protons (exception made for N– CH_2 in the α -position), and polar head N– CH_3 and N– CH_2 protons.⁴¹ Two additional peaks of lower intensity were detected around 4.5 and 7.2 ppm for CTAB/HCl and 6.0 ppm for CTAB/OH. They certainly belong to surface silanols and/or surface water species. This will be discussed later.

Silica–Surfactant Interfaces. ^1H – ^{29}Si -HETCOR Experiments. 2-D $^{29}\text{Si}\{^1\text{H}\}$ CP heteronuclear correlation (HETCOR) experiments were recorded at two different contact times ($t_{\text{CP}} = 500 \mu\text{s}$ and 5ms) to probe the through-space proximities between ^1H and ^{29}Si sites (Figure 1). No specific thermal treatment was applied to the samples prior to these experiments.

(40) Brinker, C. J.; Scherer, G.W. *Sol–Gel Science: The Physics and Chemistry of Sol–Gel Processing*; Academic Press, Inc.: San Diego, 1989.

(41) Alonso, B.; Harris, R. K.; Kenwright, A. M. *J. Colloid Interface Sci.* **2002**, *251*, 366.

CTAB/HCl Sample. The experiment performed at $t_{CP} = 500 \mu\text{s}$ is shown in Figure 1a. The 1-D projection of the ^{29}Si MAS NMR signal along the F_2 dimension shows that almost only Q_3 sites were detected at short contact times. Interestingly, the main cross-peak (A) represents a correlation between Q_3 silicon sites ($\delta = -100.9$ ppm) and protons at 7.2 ppm that confirms its assignment to Si–OH protons. The other cross-peak (B) corresponds to a correlation between Q_3 sites and N–CH $_x$ ($x = 2, 3$) protons belonging to the surfactant polar head group ($\delta = 3.3$ ppm). Its lower intensity, as compared to A, can be explained by a longer Si \cdots H distance and by the higher mobility of polar head groups, two factors that contribute to a decrease in the efficiency of the polarization transfer between ^1H and ^{29}Si nuclei. The presence of a weak cross-peak (C) between Q_4 sites ($\delta = -110.0$ ppm) and N–CH $_x$ protons is the signature of a longer distance between those species.

The experiment was repeated with $t_{CP} = 5$ ms (Figure 1b). Here, the 1-D projection of the ^{29}Si signal shows Q_3 as well as Q_4 and even Q_2 sites. New cross-peaks are now present. A weak one (E) is due to the Si(OH) $_2$ species. Its absence in the previous experiment, despite short Si \cdots H distances, is certainly related to a lack of sensitivity of the experiment to detect minor species. More interesting is the presence of the cross-peak (F) between Q_3 and protons in the alkyl chain at 1.3 ppm (presumably close to the polar head groups (β or γ positions)), together with the strong increase in intensity of the cross-peak (C). These observations demonstrate that a contact time of 5 ms allows exploring longer Si \cdots H distances. Cross-peaks A and B are still observed but with reverse intensity. Additionally, a cross-peak (D) appears between Q_3 and protons at 4.6 ppm, a value that will be related later on to the presence of mobile water molecules in weak interaction with Si–OH sites.

$^{29}\text{Si}\{^1\text{H}\}$ CP-HETCOR experiments were recorded with ^1H Lee–Goldburg homonuclear decoupling during contact time (CP-LG).⁴² The use of ^1H pulses under Lee–Goldburg conditions (proton irradiation is shifted in frequency to average out the ^1H homonuclear dipolar interaction)⁴³ eliminates most of the ^1H spin diffusion process that takes place during classical CP. The intensities of the cross-peaks between Si–OH and Q_3 and Q_4 are slightly higher for the CP-LG-HETCOR (see Supporting Information), which suggests that for a contact time of 5 ms, spin diffusion might occur between the protons of the Si–OH groups and the large reservoir of protons from the surfactant molecules. This will be confirmed later by 2-D $^1\text{H}\{^1\text{H}\}$ homonuclear correlation experiments.

CTAB/OH Sample. The $^{29}\text{Si}\{^1\text{H}\}$ CP-HETCOR experiment performed at $t_{CP} = 500 \mu\text{s}$ is shown in Figure 1c. The HETCOR spectrum only shows one cross-peak (B) that represents the correlation between the Q_3 sites ($\delta = -99.1$ ppm) and the N–CH $_x$ protons of the polar head groups ($\delta = 3.3$ ppm). In contrast to the previous sample, no cross-peak (A) between Q_3 sites and Si–OH protons of significant intensity is observed: this strongly suggests that Q_3 sites

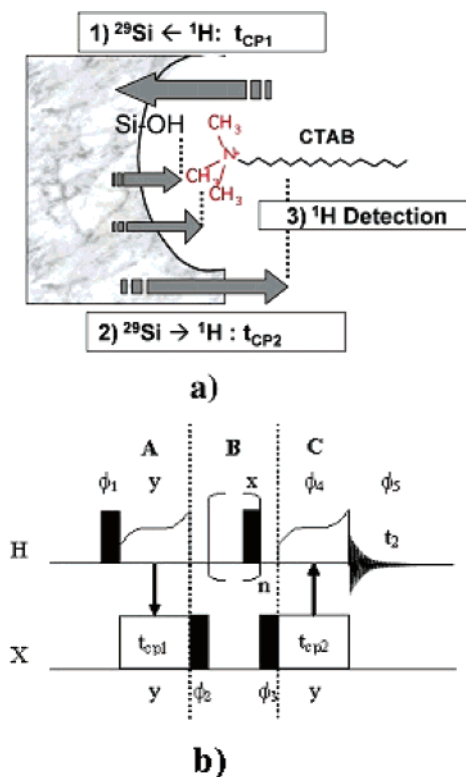


Figure 2. Schematic principle of ^1H – ^{29}Si – ^1H double CP experiment and related NMR sequence.

are primarily of the Si–O $^-$ type, rather than the Si–OH one, in agreement with the pH conditions used during the synthesis.

For a contact time $t_{CP} = 5$ ms (Figure 1d), the cross-peak (B) is still of the highest intensity, but two new cross-peaks between the Q_3 sites and protons were now observed. They were related to ^1H at $\delta = 5.7$ ppm (A) and at $\delta = 1.3$ ppm (F), respectively. The latter signal corresponds to protons belonging to the surfactant alkyl chain, CH $_2$ groups in the β or γ positions with respect to the polar head group, and it was already observed for the CTAB/HCl sample. More interesting is the cross-peak (A) that can be assigned to water molecules hydrogen bonded to Si–OH groups. Its non-observation at lower contact time is in agreement with high mobility, like protons in rapid exchange between surface Si–O $^-$ or Si–OH groups. Similar results have already been shown in the literature.⁴⁴ As for the Q_4 sites ($\delta = -109.3$ ppm), one main cross-peak was observed (C) that represents a correlation with the N–CH $_x$ protons of the polar head groups. In contrast with the CTAB/HCl sample, one cross-peak (G) was also observed between Q_4 and CH $_2$ groups of the surfactant alkyl chain, suggesting a shorter Si \cdots H distance between the corresponding species in CTAB/OH as compared to CTAB/HCl.

^1H – ^{29}Si – ^1H Double CP Experiments. The 2-D HETCOR spectra are very informative but very time-consuming (1–3 days) to record especially with a moderate magnetic field (here, 7.05 T). That is the reason why we have implemented a double cross-polarization sequence ^1H – ^{29}Si – ^1H (Figure 2)

(42) Van Rossum, B. J.; Förster, H.; De Groot, H. J. M. *J. Magn. Reson.* **1997**, *124*, 516.

(43) Lee, M.; Goldburg, W. I. *Phys. Rev.* **1965**, *140*, 1261.

(44) Gruenberg, B.; Emmler, T.; Gedat, E.; Shenderovich, I.; Findenege, G. H.; Limbach, H. H.; Buntkowsky, G. *Chem.–Eur. J.* **2004**, *10*, 5689.

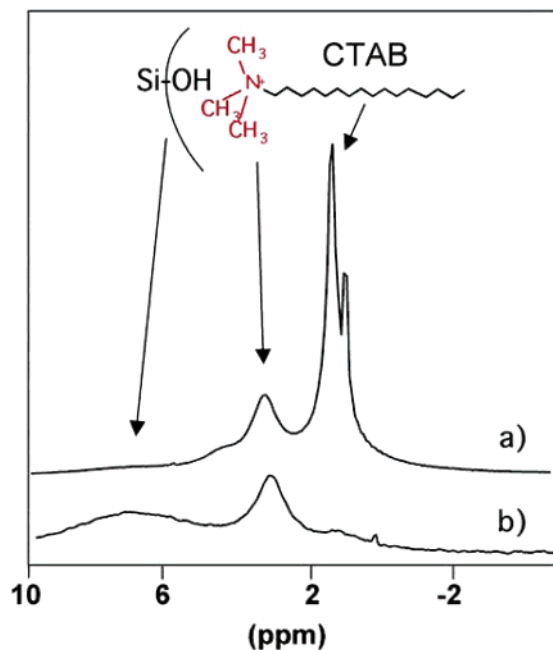


Figure 3. Comparison between the ^1H MAS NMR spectra of CTAB/HCl recorded with direct detection (a) and via the ^1H - ^{29}Si - ^1H double CP sequence with $t_{\text{CP1}} = 3$ ms and $t_{\text{CP2}} = 5$ ms (b).

to record in a 1-D experiment the ^1H NMR spectrum, equivalent to the ^1H dimension of the HETCOR experiment, but with enhanced resolution. The acquisition of each 1-D ^1H spectrum takes 1 h. The sequence consists in a first polarization transfer from ^1H to ^{29}Si (characterized by a contact time t_{CP1}), followed by a second polarization transfer back to the nearby protons (with a second contact time t_{CP2}). The first contact time was chosen to optimize the ^{29}Si signal intensity, while the second contact time was incremented to reveal progressively the type of protons characterized with increasing internuclear distances from Si sites.

Such an approach is not new in the literature since a number of pulse sequences exploiting double or multiple cross-polarization steps among two or three nuclei already exist. They are mainly used to select and enhance signals from specific nuclei in biochemical compounds.⁴⁵ Despite the large number of published sequences, we have used a different approach that is more suitable for our studied system and the desired information. The main difference between our sequence and those found in the literature concerns the process of eliminating residual proton magnetization after the first CP transfer and the consequent X nucleus protection (block B in Figure 2b). After the first CP transfer, magnetization of the X nucleus is flipped back to the $+z$ direction to be driven by the longitudinal relaxation time $T_1(\text{X})$, which is much longer than the transversal time $T_2(\text{X})$. Then, saturation of residual ^1H signals is achieved by a combination of a time-decreasing loop and $\pi/2$ pulses at the end of each loop, which was revealed to be very efficient even in the case of different ^1H transversal relaxation times, $T_2(^1\text{H})$. This

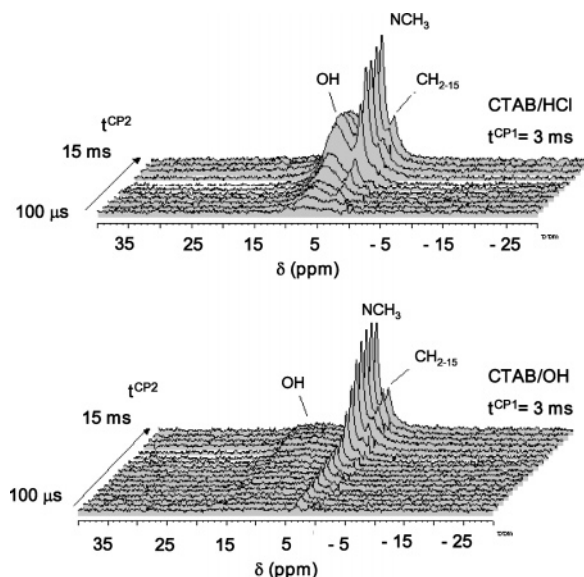


Figure 4. ^1H - ^{29}Si - ^1H double CP NMR spectra recorded on CTAB/HCl and CTAB/OH for a series of the second contact time t_{CP2} from 100 μs and 15 ms.

saturation step has two goals: suppression of all unwanted ^1H signals and, within the model of thermal reservoirs,⁴⁶ transformation of the proton bath into a hot reservoir into which magnetization can be back-transferred from the cold reservoir composed of X nuclei. After that, X magnetization is flipped back into the transversal plane before the second CP transfer. As we will see, the sequence was revealed to be quite sensitive for our systems with results comparable and complementary to the previously used 2-D HETCOR techniques. The main drawback is the need for long relaxation times T_1 for the X nucleus, but this is fully satisfied in our systems for which $30 \text{ s} \leq T_1(^{29}\text{Si}) \leq 100 \text{ s}$. Figure 3 demonstrates the efficiency of the technique to detect the protons, close to the silica surface through the comparison of the ^1H MAS NMR spectra of CTAB/HCl acquired either via direct ^1H signal detection (Figure 3a) or through the ^1H - ^{29}Si - ^1H double CP sequence (Figure 3b). The protons at 7.2 ppm due to Si-OH are clearly visible with the new sequence as well as the $\text{N}(\text{CH}_3)_3$ protons due to the polar head groups, while those due to the surfactant chains, which indeed constitute the major part of the proton bath, are hardly detected.

Figure 4 shows a comparison between the ^1H - ^{29}Si - ^1H double CP experiments recorded on CTAB/HCl and CTAB/OH for a series of the second contact time t_{CP2} . These experiments were recorded after a thermal treatment of the samples overnight at 100 $^\circ\text{C}$ to minimize the presence of adsorbed water. The value of t_{CP1} (3 ms) was chosen to optimize the polarization of the ^{29}Si nuclei after the first transfer, and it primarily concerns the Q₃ sites. The spectra for CTAB/HCl show a rather broad peak around 7 ppm due to Si-OH groups, for short t_{CP2} (100 μs). Its intensity increases with t_{CP2} reaching a maximum value of 5 ms, before a decrease in intensity due to $T_{1\rho}(^1\text{H})$ relaxation effects. On the contrary, the spectra of CTAB/OH show no similar signal; one can only notice an undefined broad signal ranging from 5 to 15 ppm that may be related to some type of OH

(45) (a) Seidel, K.; Etkorn, M.; Sonnenberg, L.; Griesinger, C.; Sebald, A.; Baldus, M. *J. Phys. Chem. A* **2005**, *109*, 2436. (b) Mulder, F. M.; Heinen, W.; van Duin, M.; Lugtenburg, J.; de Groot, H. J. M. *J. Am. Chem. Soc.* **1998**, *120*, 12891. (c) Paulson, E. K.; Morcombe, C. R.; Gaponenko, V.; Danchev, B.; Byrd, R. A.; Zilm, K. W. *J. Am. Chem. Soc.* **2003**, *125*, 15831.

(46) Yannoni, C. S. *Acc. Chem. Res.* **1982**, *15*, 201.

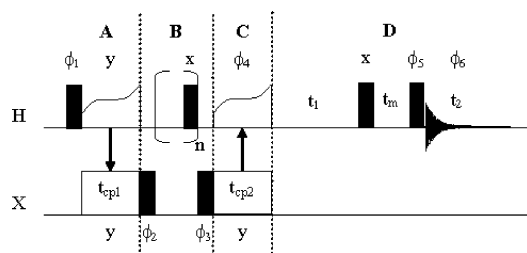


Figure 5. Pulse sequence for the 2-D ^1H homonuclear correlation spectra shown in Figure 6: ^1H -X- ^1H double CP experiment combined with a ^1H magnetization exchange experiment characterized by the mixing time τ_m .

group. This signal can be related to the peak observed at ≈ 10.5 ppm in high silica zeolites templated with trimethylalkylammonium compounds.⁴⁷ This peak was assigned to silanols hydrogen bonded to a siloxy group, $\text{SiO}^-\cdots\text{HOSi}$, with an $\text{O}\cdots\text{O}$ distance of ≈ 2.7 Å. This weak signal in the CTAB/OH sample confirms the low content in Si–OH groups. One remarkable feature in the spectral evolution is the appearance of the signal at 3.3 ppm due to the $\text{N}(\text{CH}_x)$ polar head protons. It is already detected at $t_{\text{CP}2} = 100$ μs for CTAB/OH, while for CTAB/HCl, it appears only for $t_{\text{CP}2} \geq 300$ μs . Then, for both samples, the detection of a signal at 1.3 ppm related to the CH_2 groups of the surfactant chain occurs at much longer times (≥ 7 ms).

The ^1H - ^{29}Si - ^1H double CP sequence proves thus to be very efficient to discriminate the various ^1H families depending on their distance from the Si sites. The possibility to record in a reasonable time a series of spectra at increasing contact times leads to valuable information regarding the spatial distribution of the species at the silica–surfactant interface. However, the 1-D nature of the experiment prevents a neat identification of the Si sites involved in the polarization transfer. We have first investigated the possibility of extending this sequence to a 2-D ^1H - $\{^{29}\text{Si}\}$ CP-HETCOR correlation experiment by insertion of a time increment, t_1 , after the block B. This new sequence is analogous to the ^{29}Si - $\{^1\text{H}\}$ CP-HETCOR experiment shown previously, except that the detection channel is now ^1H and no longer ^{29}Si . Consequently, we could expect to gain in resolution on the ^1H dimension, and this could be of great interest since the resolution on the indirect F_1 dimension is always limited by the number of acquirable spectra. A comparison between the two sequences recorded with similar experimental parameters shows very similar results.⁴⁸

The sequence has also been modified (Figure 5) by coupling the ^1H - ^{29}Si - ^1H double CP block with a ^1H magnetization exchange experiment. This allows us to see how the ^1H magnetization that has been selected via the ^1H - ^{29}Si - ^1H double CP can be exchanged during a mixing time τ_m within the proton spin systems. Figure 6 compares experiments recorded for three different mixing times on CTAB/HCl. For $\tau_m = 140$ μs (Figure 6a), only diagonal peaks were present, showing no magnetization exchange between the three ^1H spin systems: Si–OH groups, polar head groups, and surfactant chains. For $\tau_m = 1$ ms (Figure 6b), two cross-peaks appear: A shows a correlation between Si–OH and

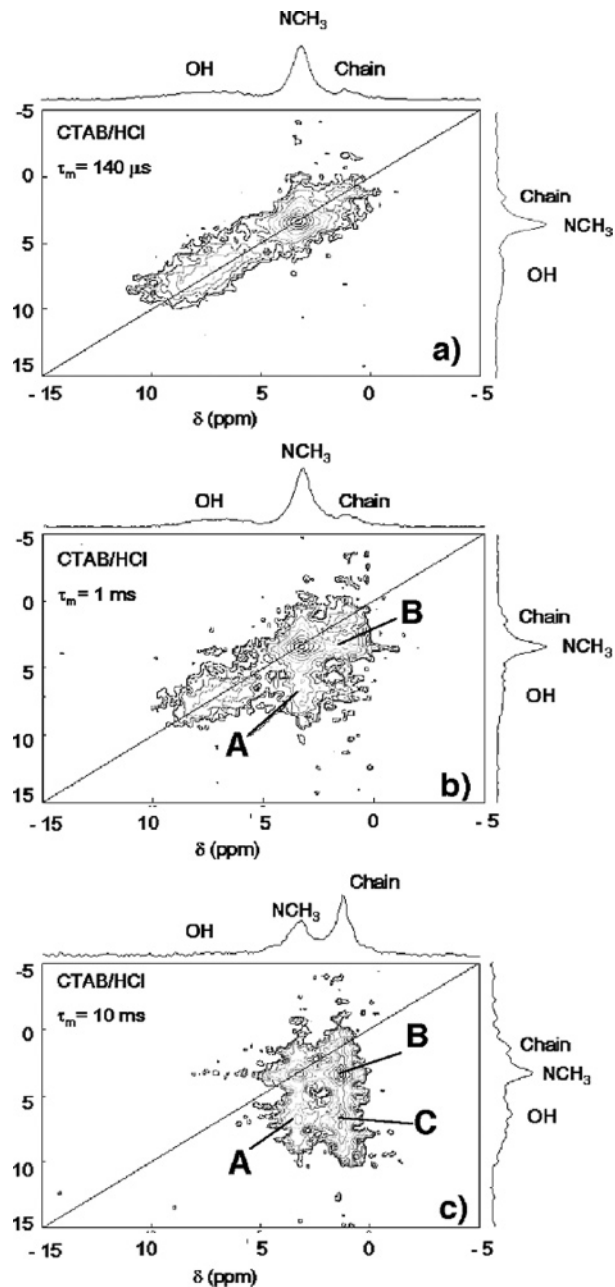


Figure 6. 2-D homonuclear ^1H correlation spectra of CTAB/HCl taken using the pulse sequence shown in Figure 5, with various mixing times: (a) $\tau_m = 140$ μs , (b) $\tau_m = 1$ ms, and (c) $\tau_m = 10$ ms.

the NCH_x groups, while B corresponds to a correlation between the NCH_x groups and the protons of the chain. For $\tau_m = 10$ ms (Figure 6c), the diagonal peak due to the Si–OH groups disappeared, and now a new cross-peak (C) is present between these Si–OH groups and the protons of the chain. By increasing the mixing time, the magnetization was progressively transferred from the surface silanols to the interior of the micelle. The fact that the transfer was going one way was a consequence of the filtering effect of the ^1H - ^{29}Si - ^1H double CP block, which polarized primarily the Si–OH and polar head protons, with almost nothing on the protons of the surfactant chain. The magnetization will thus be transferred along the following pathway: Si–OH \rightarrow polar head \rightarrow chain.

Characterization of the Surface Species. ^1H MAS NMR. To better identify the surface species, the samples were

(47) Koller, H.; Lobo, R. F.; Burkett, S. L.; Davis, M. E. *J. Phys. Chem.* **1995**, *99*, 12588.

(48) See Supporting Information (Figure S2).

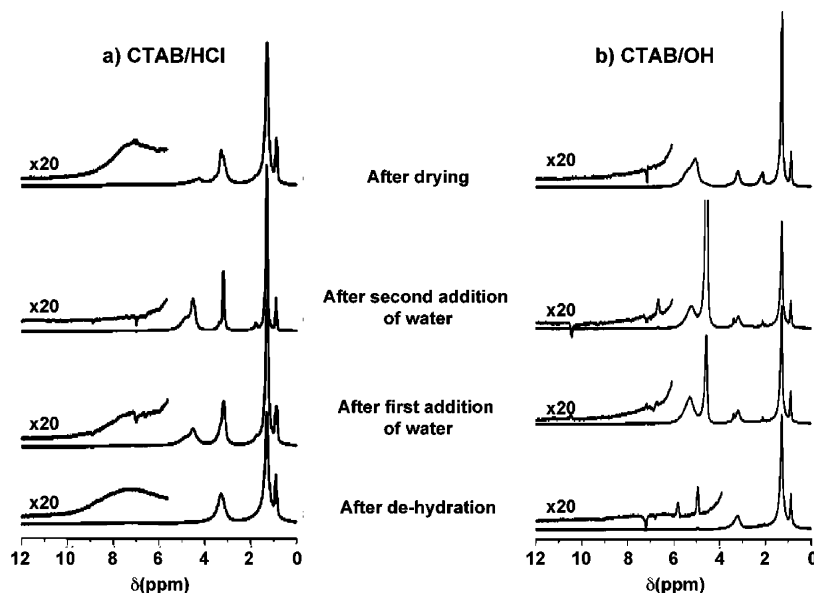


Figure 7. ^1H NMR-MAS spectra of CTAB/HCl (a) and CTAB/NaOH (b). (B_0 : 9.4 T and sample spinning: 30 kHz)

dehydrated for 24 h under vacuum ($\sim 10^{-2}$ mbar) at 100 °C. The rotors were filled in a dry glovebox, and then water was added to the rotor to follow the rehydration process of the powders. These experiments were performed with an MAS spinning rate of 30 kHz to obtain better spectral resolution.

CTAB/HCl Sample. Besides the three peaks at $\delta_{\text{iso}} = 0.9$, 1.3, and 3.3 ppm assigned to the surfactant molecules, and that have been already described, the spectrum of the dehydrated CTAB/HCl sample (Figure 7a) shows an additional broad signal of low intensity centered around 7.2 ppm. Similar chemical shift values were reported for fairly acidic protons or silanols in strong H-bonding^{24,49,50} in contrast to isolated silanols that were characterized by resonance peaks around 1–2 ppm.⁵¹ Indeed, this value is in perfect agreement with the ^1H chemical shift value found in the $^{29}\text{Si}\{^1\text{H}\}$ -HETCOR spectrum for the cross-peak assigned to the Si–OH groups of the Q_3 sites. When 1 mg of water was added to the powder, a new signal appeared that could be decomposed into two peaks: a broad one at 4.8 ppm and a sharper one at 4.5 ppm. After a second addition of water (0.8 mg), the area of the 4.8 ppm peak did not change much, while the area of the 4.5 ppm peak increased by 3 times. The peak at 4.8 ppm can be assigned to H_2O molecules in strong H-bonding with surface Si–OH groups.²⁷ The second peak could be due to H_2O molecules as well, but in weaker interaction. Interestingly, with water addition, the signals due to the surfactant sharpen especially those due to the protons of the polar head. This is a result of an increasing mobility and suggests that water molecules reached the interfacial silica–surfactant layer. The rotor was then placed under an IR lamp for 15 min of drying. The resulting ^1H spectrum was quite similar to the starting one obtained after dehydra-

tion, with even the reappearance of the peak at 7.2 ppm that progressively broadened and shifted during water addition.

CTAB/OH Sample. In contrast to the CTAB/HCl sample, the ^1H MAS NMR spectrum of dehydrated CTAB/OH (Figure 7b) hardly showed any detectable signal around 6–8 ppm, due to surface silanols in perfect consistency with the double CP results. After water addition (2.4 mg), two new signals could be identified, one rather broad at 5.3 ppm and one sharp at 4.6 ppm. Further water addition (1.4 mg) did not cause any important modification of the spectrum, besides the increase in intensity of the peak at 4.6 ppm, which was clearly due to highly mobile H_2O molecules, while the peak at 5.3 ppm could be assigned to H-bonded molecules. Further drying of the powder causes the total disappearance of the sharp peak, consistent with its assignment to free water molecules. But, the signal around 5.3 ppm was still present and presented several components. In contrast to the CTAB/HCl sample, a rather intense peak due to the H-bonded H_2O was still present, which could suggest a certain difficulty for the water molecules to escape from the interfacial zone if we consider a strong interaction between water molecules and surface silanols.

FT-IR and FT-NIR Experiments. Figure 8a shows the FT-IR absorption spectra, in the 4000–450 cm^{-1} range, of the CTAB/HCl (gray line) and CTAB/OH (black line) samples. The spectra have been normalized with respect to the intensity of the 1050 cm^{-1} band. This main intense band is assigned to Si–O–Si antisymmetric stretching modes⁵² and is accompanied by the symmetric stretching and rocking bands around 800 and 450 cm^{-1} , respectively, which represent the signature of the silica network (see Table 2 for the band assignments). The 1050 cm^{-1} vibrational mode was accompanied by another band around 1230 cm^{-1} that was assigned to the antisymmetric longitudinal optical mode (LO_3).⁵² A sharp intense band was present at 1160 cm^{-1} ; this band was overlapped with the silica stretching band at 1050 cm^{-1} and can be clearly observed in the CTAB/HCl

(49) Wolf, I.; Gies, H.; Fyfe, C. A. *J. Phys. Chem. B* **1999**, *103*, 5933.
 (50) Shenderovich, I. G.; Buntkowsky, G.; Schreiber, A.; Gedat, E.; Sharif, S.; Albrecht, J.; Golubev, N. S.; Findenegg, G. H.; Limbach, H. H. *J. Phys. Chem. B* **2003**, *107*, 11924.
 (51) Bronnimann, C. E.; Zeigler, R. C.; Maciel, G. E. *J. Am. Chem. Soc.* **1988**, *110*, 2023.

(52) Innocenzi, P. *J. Non-Cryst. Solids* **2003**, *316*, 309.

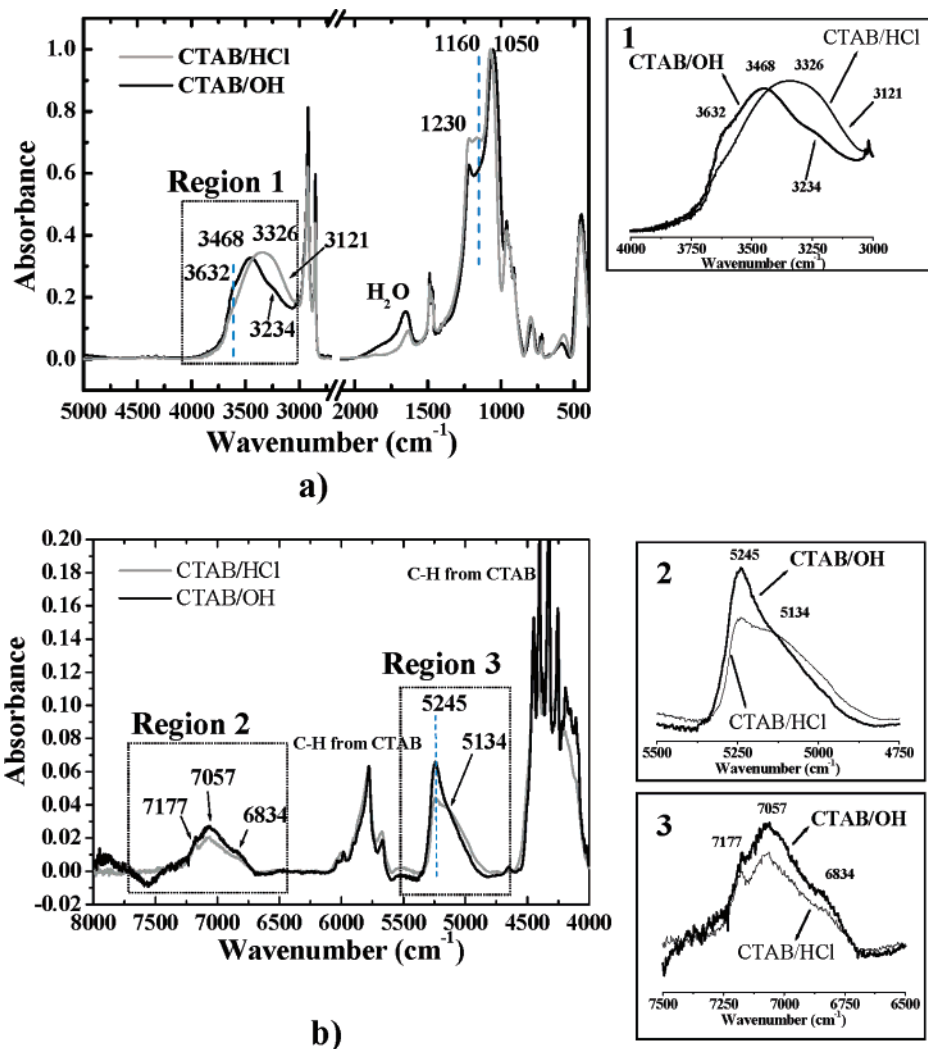


Figure 8. Infrared (a) and near-infrared (b) spectra recorded on CTAB/HCl and CTAB/NaOH.

Table 2. Assignments of Bands Present in FT-IR and NIR Spectra of CTAB/HCl and CTAB/NaOH

| IR (cm ⁻¹) | assignments | NIR (cm ⁻¹) | assignments |
|------------------------|--|-------------------------|--|
| 580, 1160 | cyclic species, cubic octameric silica cages | 4000–4500 | C–H from CTAB |
| 1050 | AS–TO ₃ stretching | 5130 | $\nu_{\text{OH}} + \delta_{\text{HOH}} (S'_1, S'_2)$ |
| 1230 | AS–LO ₃ stretching | 5245 | $\nu_{\text{OH}} + \delta_{\text{HOH}} (S'_0)$ |
| 1630 | adsorbed water | 5500–6000 | C–H from CTAB |
| 2700–3000 | C–H from CTAB | 6834 | $2\nu_{\text{OH}} (S'_1, S'_2)$ |
| 3121 | OH stretching | 7057 | $2\nu_{\text{OH}} (S'_0)$ |
| 3234 | H-bonded water | 7177 | $2\nu_{\text{OH}} (S'_0)$ |
| 3326 | H-bonded Si–OH chains | | |
| 3468 | H-bonded Si–OH chains | | |
| 3632 | terminal silanols | | |

sample but not in CTAB/OH. The presence of this band can be correlated to the presence of cyclic or cage-like silica-based species or disordered induced modes.⁵³ Even if a specific attribution requires a detailed investigation that is beyond the purpose of this work, we can, however, deduce that this mode is an indication of different structural features present in the silica backbone. The basic and acidic synthesis produced structural differences, as also indicated by the band at 580 cm⁻¹, which were due to 4-fold silica rings⁵⁴ and were more intense in the CTAB/OH sample. The presence of the

1160 cm⁻¹ band in CTAB/HCl certainly accounts for a different nature of the silica structure with respect to CTAB/OH.

Another informative band was observed at 1640 cm⁻¹ ($\nu_{\text{b}}(\text{H}_2\text{O})$); this band is assigned to molecular water and clearly shows that the water content in CTAB/OH is higher than in CTAB/HCl. The bands between 2700 and 3000 cm⁻¹ were due to the C–H stretching vibrations from the surfactant molecules and are related with the corresponding deformation bands between 1400 and 1500 cm⁻¹.⁵⁵ The region between 3000 and 3600 cm⁻¹ corresponds to the O–H stretching

(53) (a) Innocenzi, P.; Falcaro, P.; Grosso, D.; Babonneau, F. *J. Phys. Chem. B* **2003**, *107*, 4711. (b) Kirk, C. T. *Phys. Rev. B* **1988**, *38*, 1255.

(54) Yoshino, H.; Kamiya, K.; Nasu, H. *J. Non-Cryst. Solids* **1990**, *126*, 68.

(55) Ryczkowski, J.; Goworek, J.; Gac, W.; Pasieczna, S.; Borowiecki, T. *Thermochim. Acta* **2005**, *434*, 2.

vibrations from silanols and water species. The wide band was formed by several overlapped vibrational modes, and in general, a detailed attribution requires complex deconvolution methods. The spectra show, however, some distinctive features that can give some valuable information. The first one is related to the pore surface; the spectra suggest, in fact, the presence of longer H-bonded chains due to adsorbed water and surface silanols in CTAB/HCl with respect to CTAB/OH. The maximum falls, in fact, around 3326 cm^{-1} for CTAB/HCl instead of 3468 cm^{-1} for CTAB/OH; furthermore, the band appears sharper, which is an indication of shorter silanol chains. The shoulder appearing at 3632 cm^{-1} mainly in CTAB/OH sample indicated the presence of terminal silanols with a weaker H-bonding character. Their presence can be associated to a higher degree of condensation in CTAB/OH. In both samples, we note the absence of a peak due to isolated surface silanols around 3750 cm^{-1} .

In the OH stretching region, the presence of molecular water can be followed using the first overtone of the bending mode of H-bonded water ($2\nu_b$), which falls around 3200 cm^{-1} . The broadness of the HCl band, which overlaps the $2\nu_b$ band of water, does not allow, however, a direct comparison between the two samples.

Bands in the NIR region (Figure 8b) account for the first overtones of $\nu(\text{OH})$ stretching vibrations between 6800 and 7300 cm^{-1} and combinations of $\nu(\text{OH})$ and $\delta(\text{HOH})$ vibrations between 5000 and 5300 cm^{-1} . CH groups from CTAB resonate in the 5500 – 6000 and 4000 – 4500 cm^{-1} regions, and they will not be discussed here. The various types of water molecules interacting with the surface of silica have been discussed in a publication from Perry and Li⁵⁶ in terms of the S'_0 , S'_1 , and S'_2 species. S'_0 corresponds to a water molecule bonded to a silanol group through an oxygen atom; S'_1 corresponds to a water molecule bound to a SiOH group via oxygen and is hydrogen bonded to one other water molecule; and S'_2 corresponds to a water molecule bound to a SiOH group via oxygen and is hydrogen bonded to two water molecules. Bands due to combinations of $\nu(\text{OH})$ and $\delta(\text{HOH})$ vibrations are expected at 5285 and 5128 cm^{-1} for S'_0 and (S'_1 , S'_2), respectively. A main difference is observed between CTAB/HCl and CTAB/OH samples, indicating that water molecules exhibit weaker interactions with the surface in CTAB/OH (dominant band due to S'_0) in agreement with data in the middle infrared. In the CTAB/HCl material, water tends to strongly hydrogen bond to surface silanols (bands at 5245 and 5134 cm^{-1} assigned to S'_1 and S'_2). The presence of the S'_2 water species should account for the formation of long-range H-bonded chains and multilayers at the silica surface.

Discussion

The combination of 2-D $^{29}\text{Si}\{-^1\text{H}\}$ -HETCOR and 1-D $^1\text{H}\text{-}^{29}\text{Si}\text{-}^1\text{H}$ double CP spectra clearly show different responses for CTAB/HCl and CTAB/OH. At short contact times ($500\text{ }\mu\text{s}$), only the ^1H nearest neighbors to the Q_3 sites were selected. In the CTAB/HCl material, the related high

chemical shift value ($\delta = 7.2\text{ ppm}$) suggests the high acidic character of the protons as previously discussed. The presence of some Si-OH_2^+ species along with Si-OH ones probably completes the picture of the silica surface. The only fact against a massive presence of Si-OH_2^+ species, although in perfect agreement with the synthesis conditions used for the CTAB/HCl material, is the almost 1:1 ($\text{Cl}^- + \text{Br}^-$)/ N^+ molar ratio (Table 1), indicating that charge matching with the positive charge of the polar head group, CTA^+ , is almost completely accomplished through the presence of the Cl^- counterions. Indeed, a correlation between Q_3 sites and the protons of the surfactant polar head exists, demonstrating the very close proximity between these two species despite the presence of the counterion. In the CTAB/OH sample, the absence of correlation between Q_3 sites and OH-type protons for a $500\text{ }\mu\text{s}$ contact time suggests that the majority of the Q_3 sites is composed of Si-O^- species as previously discussed in perfect agreement with initial basic conditions. Consequently, the Q_3 sites are in strong interaction with the protons of the CTA^+ polar head groups, as shown by the intense and lone correlation present in the corresponding HETCOR spectrum.

For longer contact times (5 ms), the two systems still present different behaviors, especially for the OH surface species (Si-OH as well as H_2O). In both samples, Q_3 sites strongly interact with the CTA^+ polar head protons (N-CH_x) as well as with the CH_2 groups of the surfactant chain certainly in the β or γ positions with respect to the polar head group. The main difference regarding the correlations involving the protons of the surfactant molecules is the intense cross-peak between CTA^+ polar head protons and Q_4 sites that is detected only in the CTAB/OH sample. It corresponds to a stronger $^{29}\text{Si}\text{-}^1\text{H}$ heteronuclear dipolar interaction between the $\text{N}^+(\text{CH}_3)_3$ protons and the Si surface sites that could be attributed to shorter distances existing between the positively charged polar head of the surfactant and silica walls. However, one may keep in mind that these systems cannot be considered as rigid ones. Indeed, the relatively good resolution of the ^1H MAS NMR spectra recorded at relatively low spinning frequency (14 kHz ; see Supporting Information) is clearly due to internal mobility of the constitutive species that leads to a partial averaging of the strong ^1H homonuclear dipolar coupling. This prevents a direct correlation between the CP responses and the $^{29}\text{Si}\text{-}^1\text{H}$ internuclear distances.

Important structural information that can be extracted from the $^{29}\text{Si}\text{-}^1\text{H}$ CP-based NMR experiments are the apparent differences in the OH species present at the silica-surfactant interfaces. At longer contact times (5 ms), the Q_3 sites show correlation with OH-type protons, characterized by different chemical shift values depending on the sample. In CTAB/HCl, the peak at 7.2 ppm (already detected at a short contact time) is assigned to primarily Si-OH groups and possibly some Si-OH_2^+ species. Additionally, a signal is now detected at 4.6 ppm assigned to H_2O molecules in interaction with the surface. In CTAB/OH, a ^1H resonance signal at 5.7 ppm appears. As previously hypothesized, the associated OH groups could be part of water molecules in interaction with the Si-O^- surface sites since double CP experiments

Proposed interaction model at silica surface

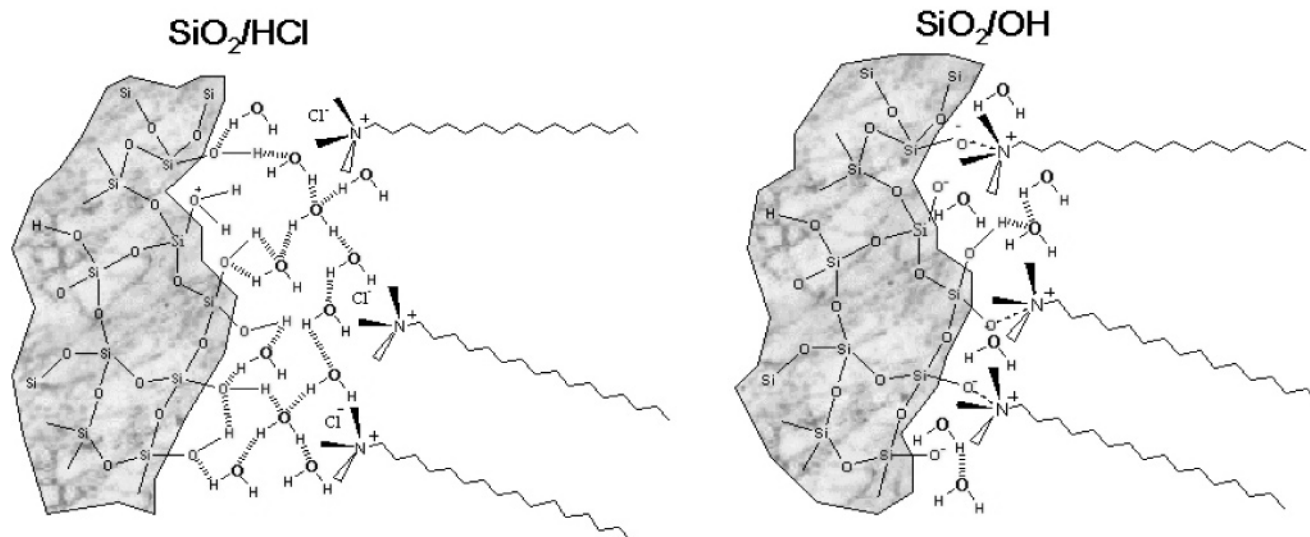


Figure 9. Schematic view of the silica–surfactant interfaces in CTAB/HCl and CTAB/NaOH samples.

performed on the dried sample do not show any explicit silanol peak.

To obtain a better description about these OH surface species, one can compare the ^1H MAS NMR experiments performed on dehydrated and partially rehydrated samples. The spectra of the dehydrated samples totally confirmed the results extracted from the ^{29}Si - ^1H CP-MAS NMR experiments with no evidence for any OH in the CTAB/OH sample and a signal at 7.2 ppm for CTAB/HCl that can be safely assigned to the Si–OH and/or SiOH_2^+ groups. Because of the dehydrated nature of the sample, one could rule out extensive H-bonding with H_2O molecules. But, the high chemical shift value could be explained by the presence of short hydrogen-bond distances between the H-atom of a Si–OH group and the O-atom of a neighboring Si–O–Si surface site.⁵⁷ When water was added to the samples, the ^1H NMR responses were completely different for both systems. In CTAB/OH, broad ($\delta = 5.3$ ppm) and a sharp ($\delta = 4.6$ ppm) distinct ^1H resonance signals were detected. The sharp one was undoubtedly due to free H_2O molecules that did not interact with the surface, if one considers the small line width of the peak. The broader one can be related to the peak at 5.7 ppm observed in the HETCOR experiment, and assigned to H-bonded H_2O molecules, certainly in interaction with Si–O $^-$ surface sites. Interestingly, after the second water addition, only the peak due to free water increased, indicating that water was no longer interacting with the surface. One possible scenario is that in the CTAB/OH sample, the interfacial space was limited to accommodate a large amount of water molecules, and this was in agreement with the strong electrostatic interaction between the CTA^+ polar head groups and the negatively charged silica walls. In the CTAB/HCl sample, no sharp signal due to free water was detected even after the second water addition, indicating that all water molecules were able to interact with the silica surface. Two

overlapped broad resonance signals at 4.8 and 4.5 ppm are now present. As previously seen, only the intensity of the peak at 4.5 ppm increased with the amount of added water. This peak was certainly due to H_2O molecules in weak interaction with the surface. However, the line width, which was larger than that in the case of CTAB/OH, suggested that the water molecules were in a confined environment and possibly in the silica surfactant interfacial layer. After the water addition steps, the peak due to Si–OH present at 7.2 ppm in the dehydrated sample seemed to progressively shift to lower chemical shift values and to broaden. This indicated possible exchange mechanisms between the Si–OH surface groups and the water molecules. Indeed, the reported chemical shift value of 4.8 ppm for the second signal indicated rather weak interactions between the water molecules and the silica surface, but certainly through extensive H-bonding.

Infrared, and more specifically near-infrared experiments, have confirmed for the two samples distinct structures for the adsorbed water layers present at the silica–surfactant interface: water molecules exhibit weaker interactions with the surface in the CTAB/OH sample, while they tend to strongly hydrogen bond to surface silanols in the CTAB/HCl sample and to form long-range H-bonded chains and multilayers at the silica surface. The presence of these water layers in CTAB/HCl accounts for the large decrease in the line width of the ^1H resonance signal at 3.3 ppm due to the protons of the polar head groups, from 150 Hz in the dehydrated sample down to 30 Hz after the second water addition. This indicated a higher mobility of the polar head groups, due to a higher solvation degree. This effect has already been discussed by Sizun et al.,⁵⁸ who used methanol to increase the CTAB mobility. On the contrary, when water was added to the CTAB/OH sample, the peak line width

(57) Gervais, C., private communication.

(58) Sizun, C.; Raya, J.; Intasiri, A.; Boos, A.; Elbayed, K. *Microporous Mesoporous Mater.* **2003**, *66*, 27.

did not vary with water addition, indicating that extensive solvation did not occur, due to strong electrostatic interactions between the polar head groups and the silica surface sites, which prevents the formation of water layers in the interfacial palisade.

All these studies can allow proposing the schemes shown in Figure 9 for the surfactant–silica interfaces in CTA⁺ templated samples prepared under acidic and basic conditions. The main difference comes from the existence of an extended network of H-bonded water molecules in the acidic case, which is certainly favored by the presence of hydrated Cl[−] counterions.

Conclusion

This work has reinvestigated the structural study of CTAB templated mesostructured silicas prepared under highly acidic and basic conditions. We have combined highly advanced 1-D and 2-D solid-state NMR methods based on ²⁹Si-¹H dipolar coupling with near-infrared spectroscopy to evidence the structural differences at the silica–surfactant interface that had been proposed through the so-called S⁺I[−] and S⁰X[−]I⁺ interaction mechanisms. Indeed, we went one step further since we have clearly identified the presence of water molecules in the interfacial region that behave differently

depending on the synthetic conditions. Silica obtained under acidic conditions showed a silanol-rich interface. Surfactant polar heads, whose charge was completely neutralized by its own counterion, settled close to the silanol palisade, although left enough room for water molecules forming an extended hydrogen-bonding network. When silica was prepared under basic conditions, the surface was rich in SiO[−] groups that were the lone source for the neutralization of the polar head charge. This direct SiO[−]/N⁺(CH₃)₃ interaction induced a close proximity between surfactant polar head group and silica surface, and it consequently prevented water molecules from largely interacting with the silica surface.

Supporting Information Available: ¹H chemical shift values for CTAB/HCl and CTAB/OH samples. ¹H NMR-MAS spectra of CTAB/HCl and CTAB/OH samples. Comparison between the classical 2-D ²⁹Si-{¹H} CP-HETCOR experiment and the 2-D ¹H-{²⁹Si} CP-HETCOR experiment recorded with a pulse sequence based on the ¹H-²⁹Si-¹H double CP sequence. For the CTAB/HCl sample, comparison between ¹H traces extracted from ²⁹Si-{¹H} CP-HETCOR and CPLG-HETCOR experiments for Q₃ (a) and Q₄ (b) sites. This material is available free of charge via the Internet at <http://pubs.acs.org>.

CM062545J